Electronic Supplementary Material (ESI) for Journal of Materials Chemistry A.

Supporting Information

Insights into the Lithiation Mechanism of CF_x by A Joint High-resolution ^{19}F NMR, *in-situ* TEM and ^{7}Li NMR Approach

Guiming Zhong,[‡, a, b] Huixin Chen,[‡, a, b] Yong Cheng,[c] Lingyi Meng,[a, b] Haodong Liu,[d] Zigeng Liu,[e] Guorui Zheng,[f] Yuxuan Xiang,[f] Xiangsi Liu,[f] Qi Li,[f] Qiaobao Zhang,[c] Hongjun Yue,[*, a, b] Canzhong Lu,[*, a, b] Yong Yang[f]

[a] CAS key Laboratory of Design and Assembly of Functional Nanostructures, and Fujian Provincial Key Laboratory of Nanomaterials, Fujian Institute of Research on the Structure of Matter, Chinese Academy of Sciences, Fujian 350002, China

[b] Xiamen Institute of Rare Earth Materials, Haixi institutes, Chinese Academy of Sciences, Xiamen, 361021, China

[c] Department of Materials Science and Engineering, Xiamen University, Xiamen361005, China

[d] Department of Nanoengineering, University of California San Diego, La Jolla, CA 92093, USA

[e] Max-Plank-Institut für Chemische Energiekonversion, Stiftstr. 34-36, 45470 Mülheim an der Ruhr, Germany

[f] State Key Lab of Physical Chemistry of Solid Surfaces, Collaborative Innovation Center of Chemistry for Energy Materials and Department of Chemistry, Xiamen University, Xiamen 361005, China

‡ These two authors contributed equally.

* Corresponding Authors. E-mail: hjyue@fjirsm.ac.cn (H. Yue); czlu@fjirsm.ac.cn (C. Lu);

1. Properties of GF_x (x= 0.5, 0.8, 1.1) and $CF_{1.0}$ materials

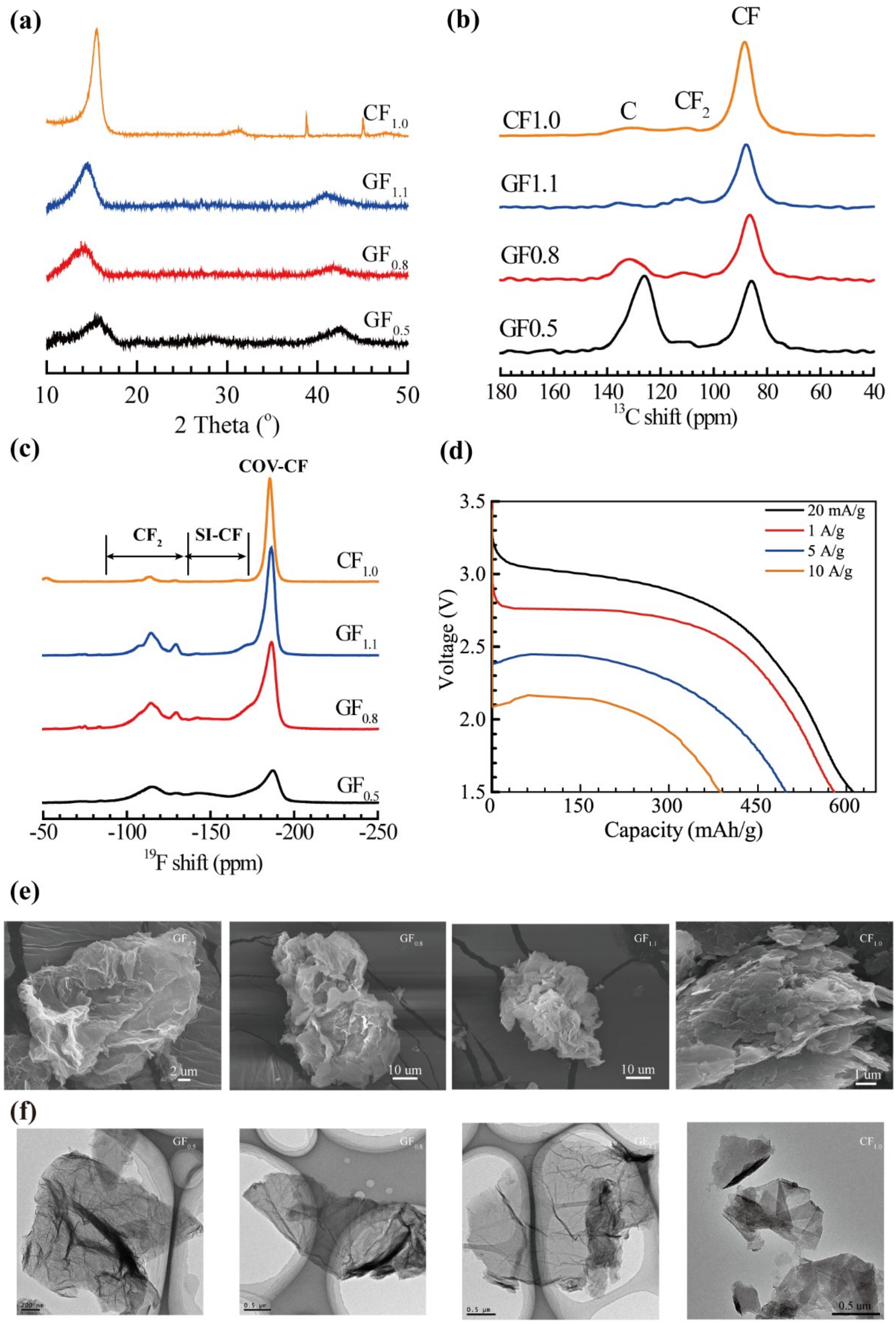

Figure S1. (a) XRD patterns, (b) ^{13}C NMR and (c) ^{19}F NMR spectra of prepared fluorinated graphene nanosheets GF_x (x = 0.5, 0.8, 1.1) and fluorinated graphite $CF_{1.0}$ materials. (d)

Discharge profiles of $GF_{0.5}$ at different current densities. SI-CF and COV-CF in Figure S1c refer to the semi-ionic and covalent CF bonds, respectively. (e) SEM and (f) TEM images of GF_x (x = 0.5, 0.8, 1.1) and $CF_{1.0}$ materials.

2. *Ex-situ* XPS spectra of $GF_{0.5}$ materials

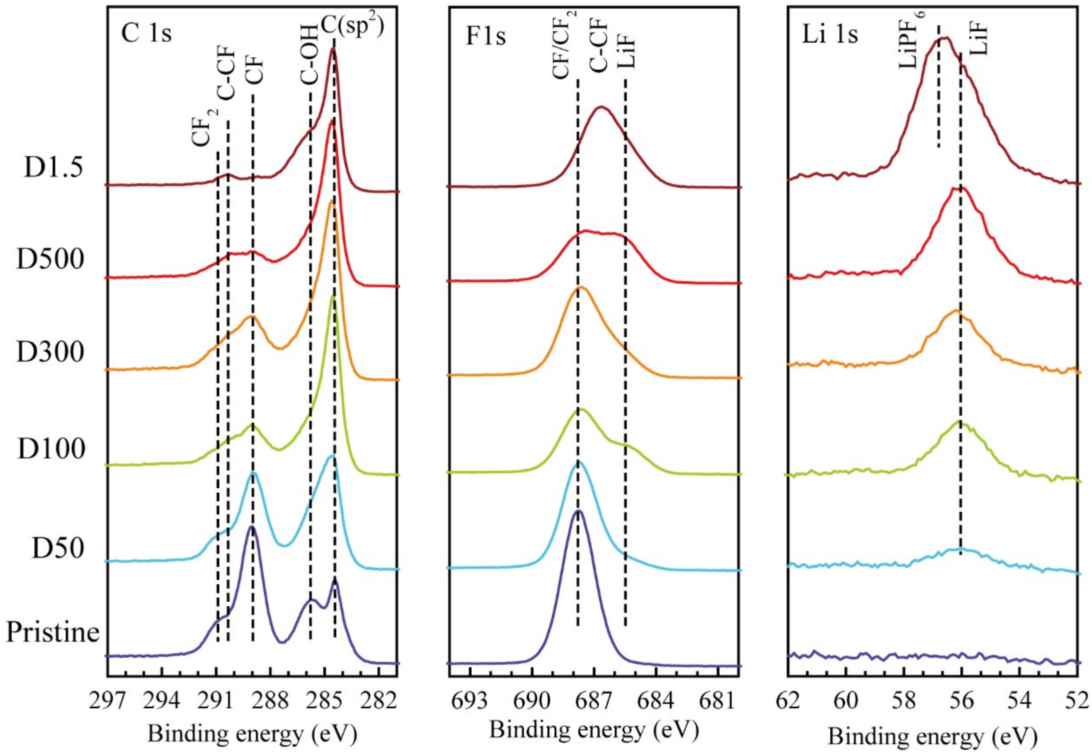

Figure S2. XPS C1s, F1s, and Li1s of $GF_{0.5}$ materials under various discharge states.

3. *Ex-situ* ^{19}F NMR results of $GF_{0.5}$ and $GF_{0.8}$ materials

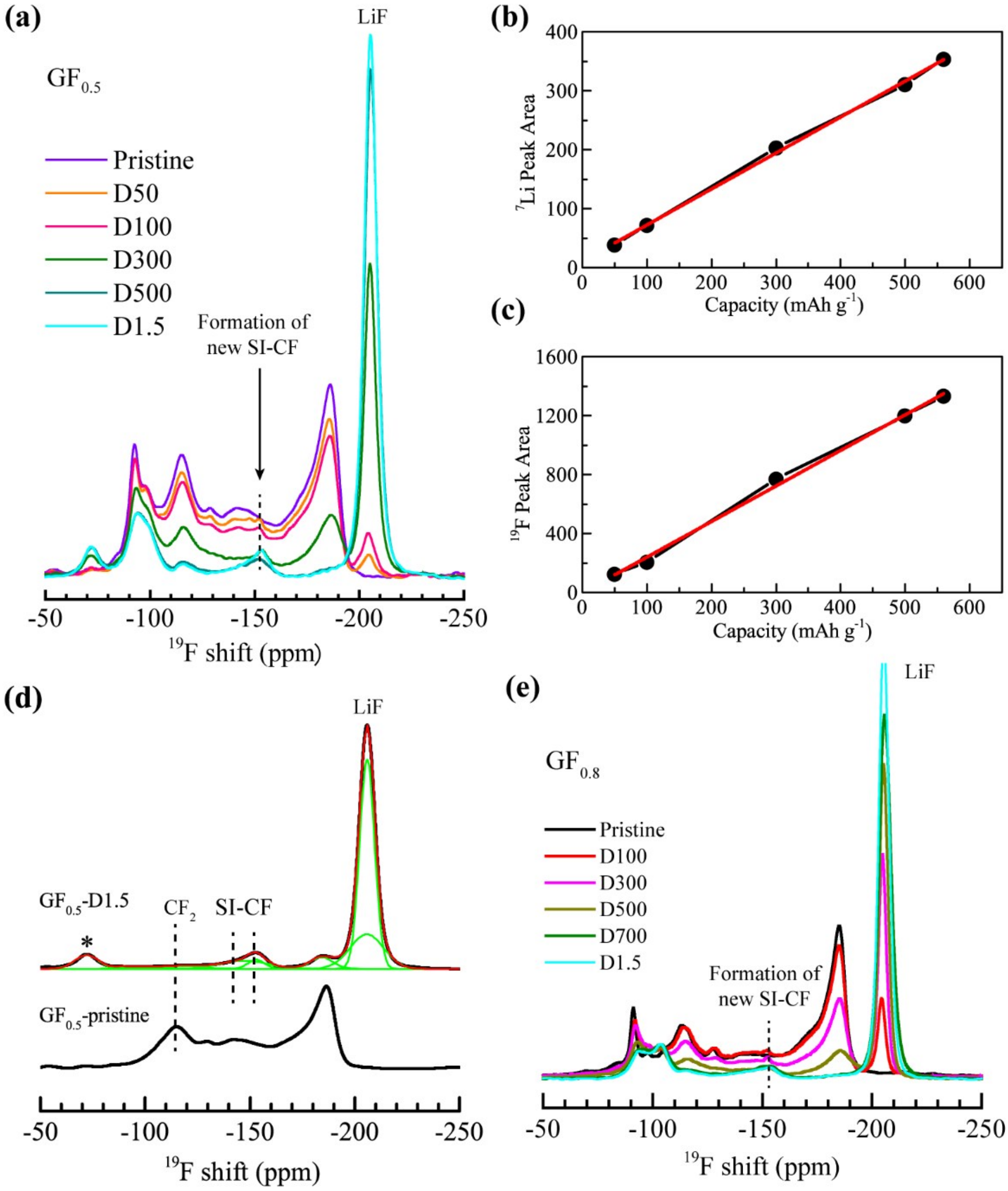

Figure S3. (a) Stack patterns of mass-normalized ^{19}F NMR spectra of the $GF_{0.5}$ electrodes (PVDF as the binder) under variable discharge states. (b) Integrated ^{7}Li peaks areas and (c) ^{19}F peaks areas of LiF signals in ^{7}Li and ^{19}F NMR spectra. (d) ^{19}F NMR spectra of $GF_{0.5}$ electrodes (sodium carboxymethyl cellulose as binder) at pristine and D1.5 states. (e) Mass-normalized ^{19}F NMR spectra of the $GF_{0.8}$ electrodes (PVDF as binder) under different discharge states.

4. *Ex-situ* ^{19}F NMR spectra and XRD patterns of $CF_{1.0}$ materials

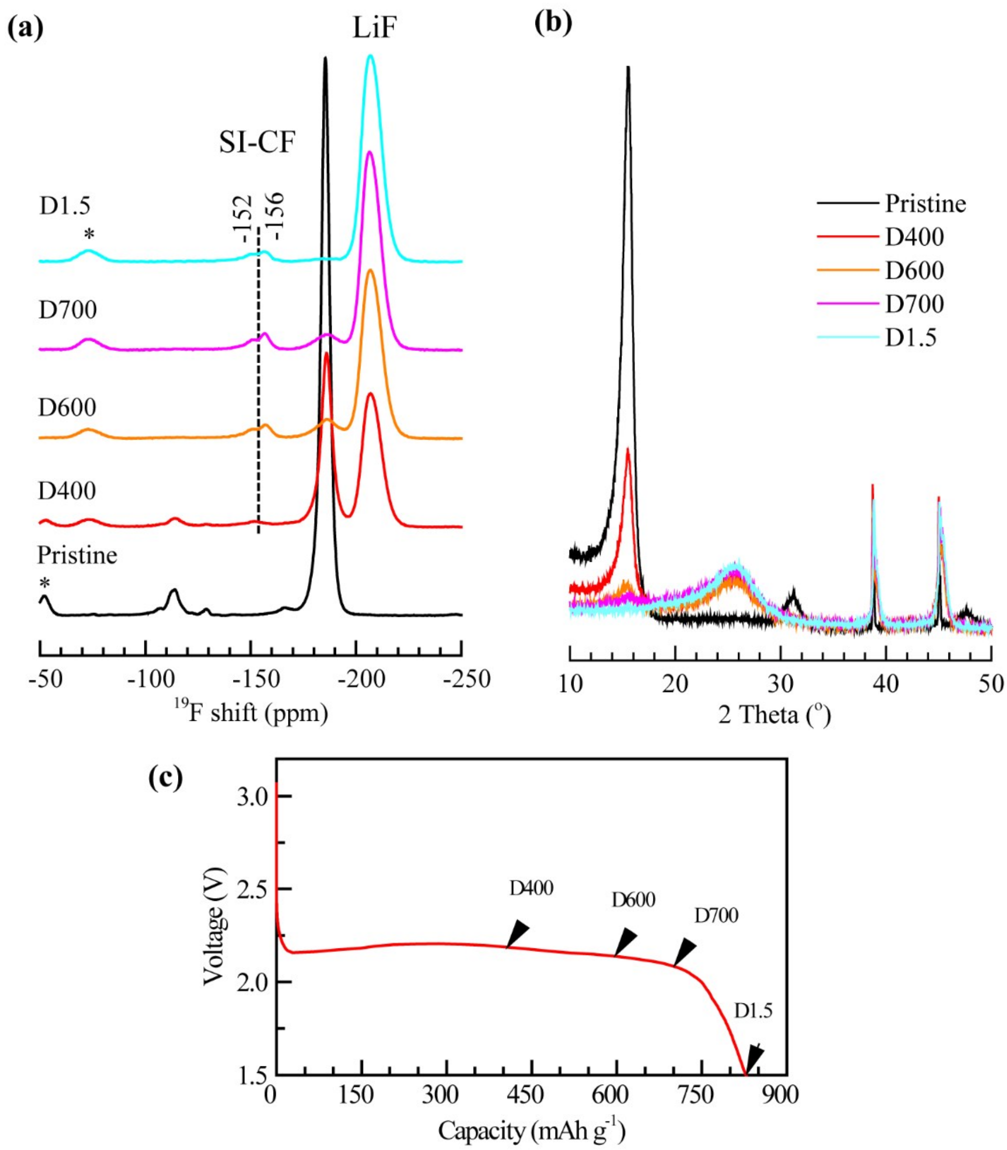

Figure S4. (a) Mass-normalized ^{19}F NMR spectra and (b) XRD patterns of $CF_{1.0}$ under variable discharge states. (c) Discharge profile of $CF_{1.0}$ at a current density of 20 mA g^{-1}. The asterisks in Figure S3a refer to the spinning sidebands.

5. Properties of reference materials GF_x (x = 0.06 - 0.22)

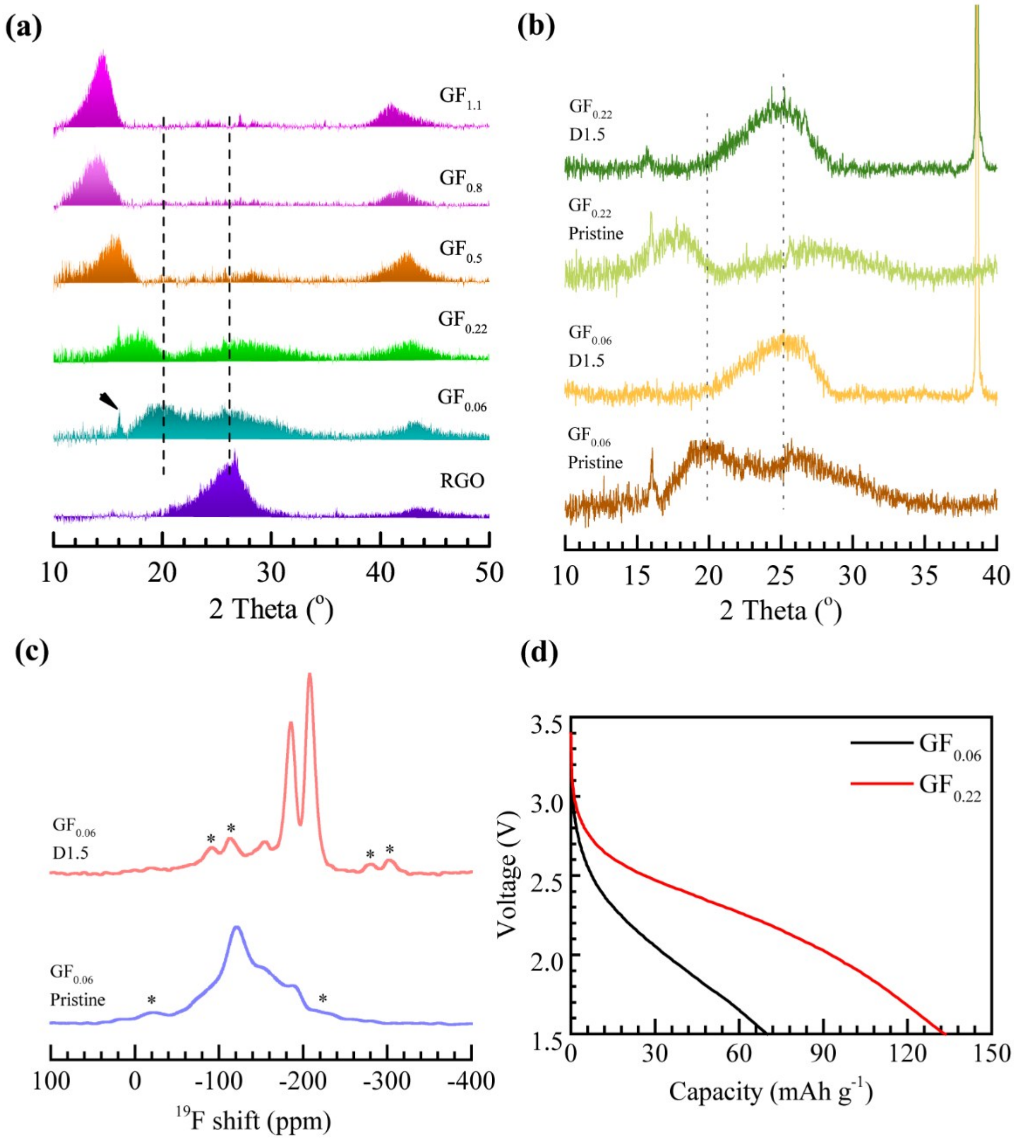

Figure S5. (a) XRD patterns of GF_x (x= 0, 0.06, 0.22, 0.5, 0.8, and 1.1) materials, and (b) $GF_{0.06}$ and $GF_{0.22}$ electrodes at pristine and D1.5 states. (c) Mass-normalized ^{19}F NMR spectra of $GF_{0.06}$ electrodes at pristine and D1.5 states acquired with spinning frequency of 35 kHz. (d) Corresponding discharge profiles of prepared $GF_{0.06}$ and $GF_{0.22}$ materials for *ex-situ* study. The asterisks in Figure S4c refer to the spinning sidebands.

6. Morphology of $GF_{0.5}$ at pristine and discharge states in solid-state batteries

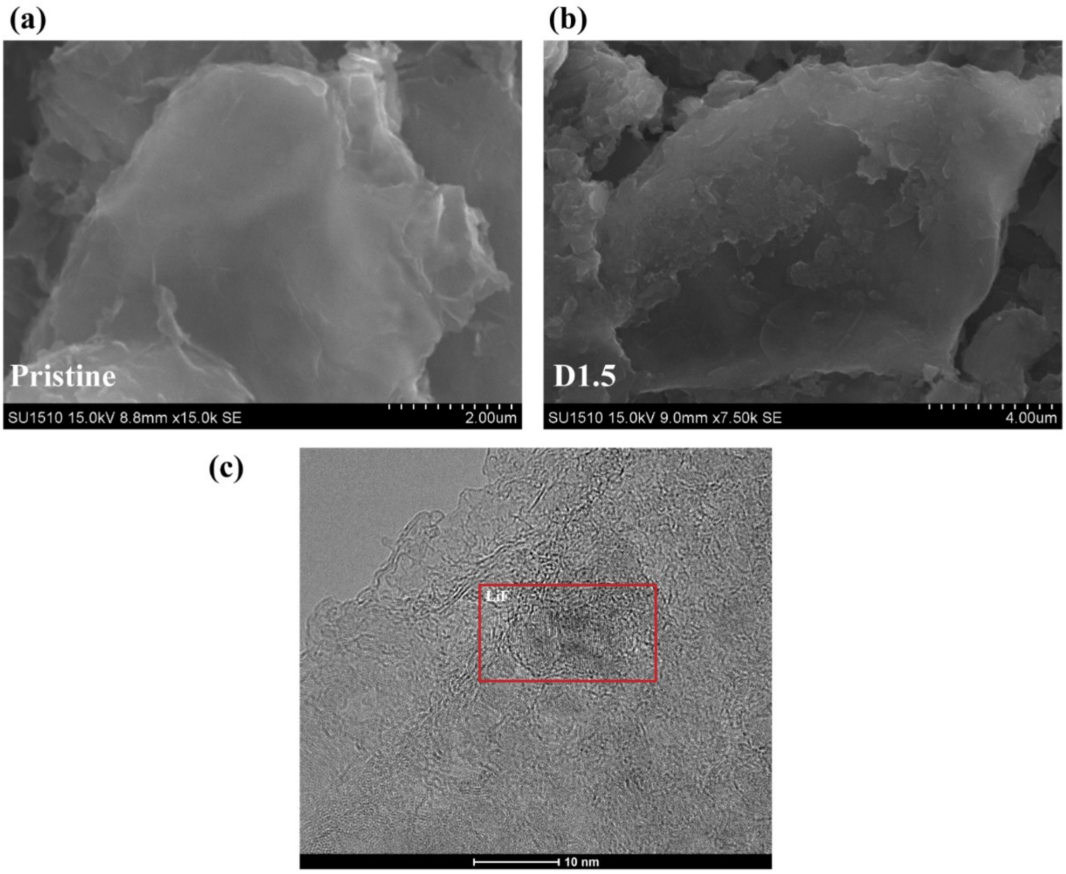

Figure S6. SEM images of (a) pristine and (b) discharged $GF_{0.5}$ materials in solid-state batteries. (c) HR-TEM image of discharged $GF_{0.5}$ material in solid-state batteries. The LiF particle is squared in red.

7. Impedance results of $GF_{0.5}$ and $GF_{0.8}$ materials during discharge

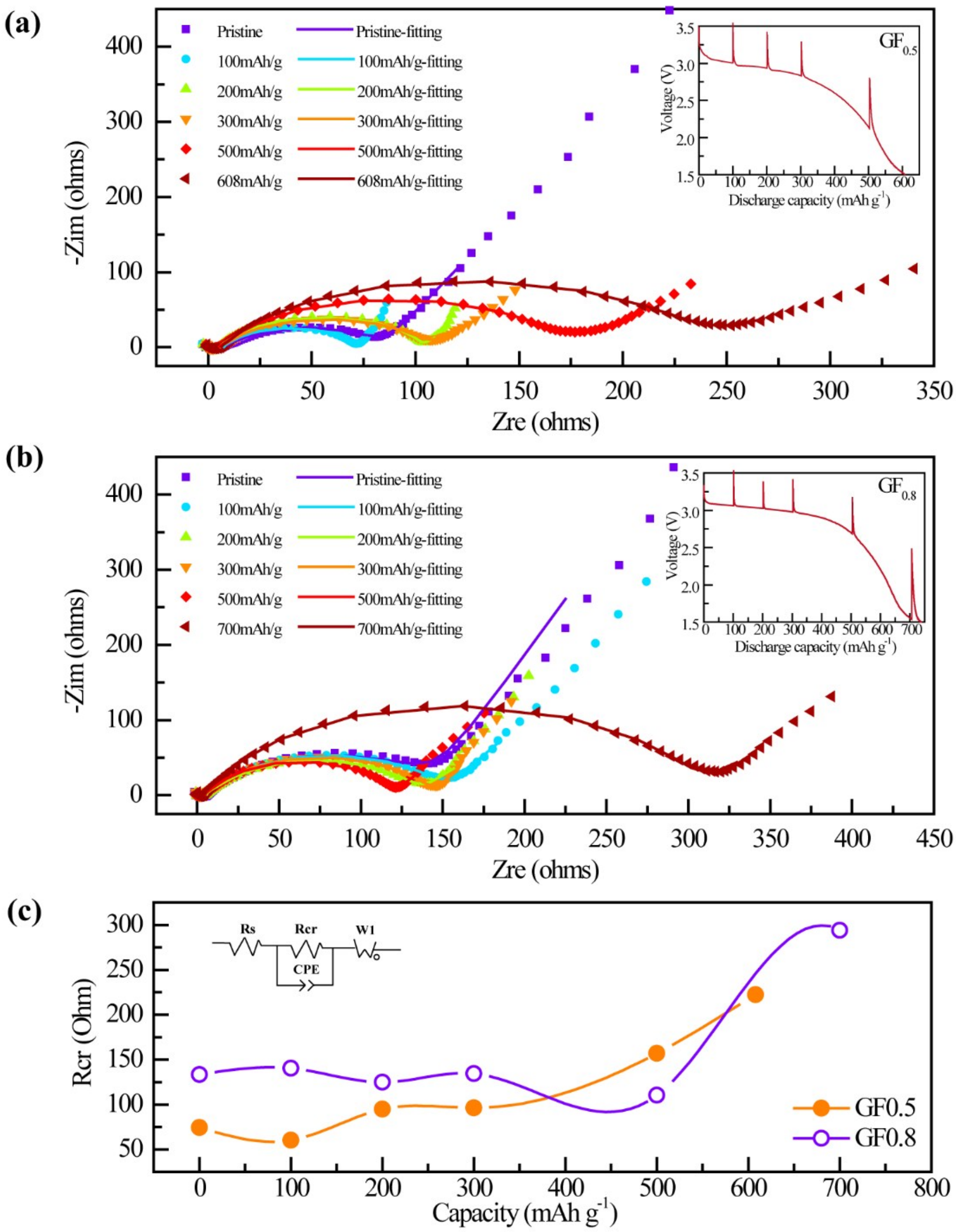

Figure S7. EIS results and the fitting plots of (a) Li/$GF_{0.5}$ battery and (b) Li/$GF_{0.8}$ battery under different discharge states. (c) Fitting R_{cr} results of EIS. R_s and R_{cr} refer to the solution resistance, and the sum of passivation layer resistance and charge-transfer resistance, respectively.

The impedance of Li/GF_x cell is fitted on the basis of the circuit diagram in Figure S7c. The impedances of solution R_s and R_{cr} (the sum of passivation layer resistance and charge-transfer resistance) are included in the fitting. Since the decomposition of electrolyte to form SEI is negligible in the first discharge process. The increasing impedance of Li/GF_x cell during discharge is mainly due to the change of GF_x cathode.

8. *In-situ* TEM device and schematics illustration of *in-situ* TEM test.

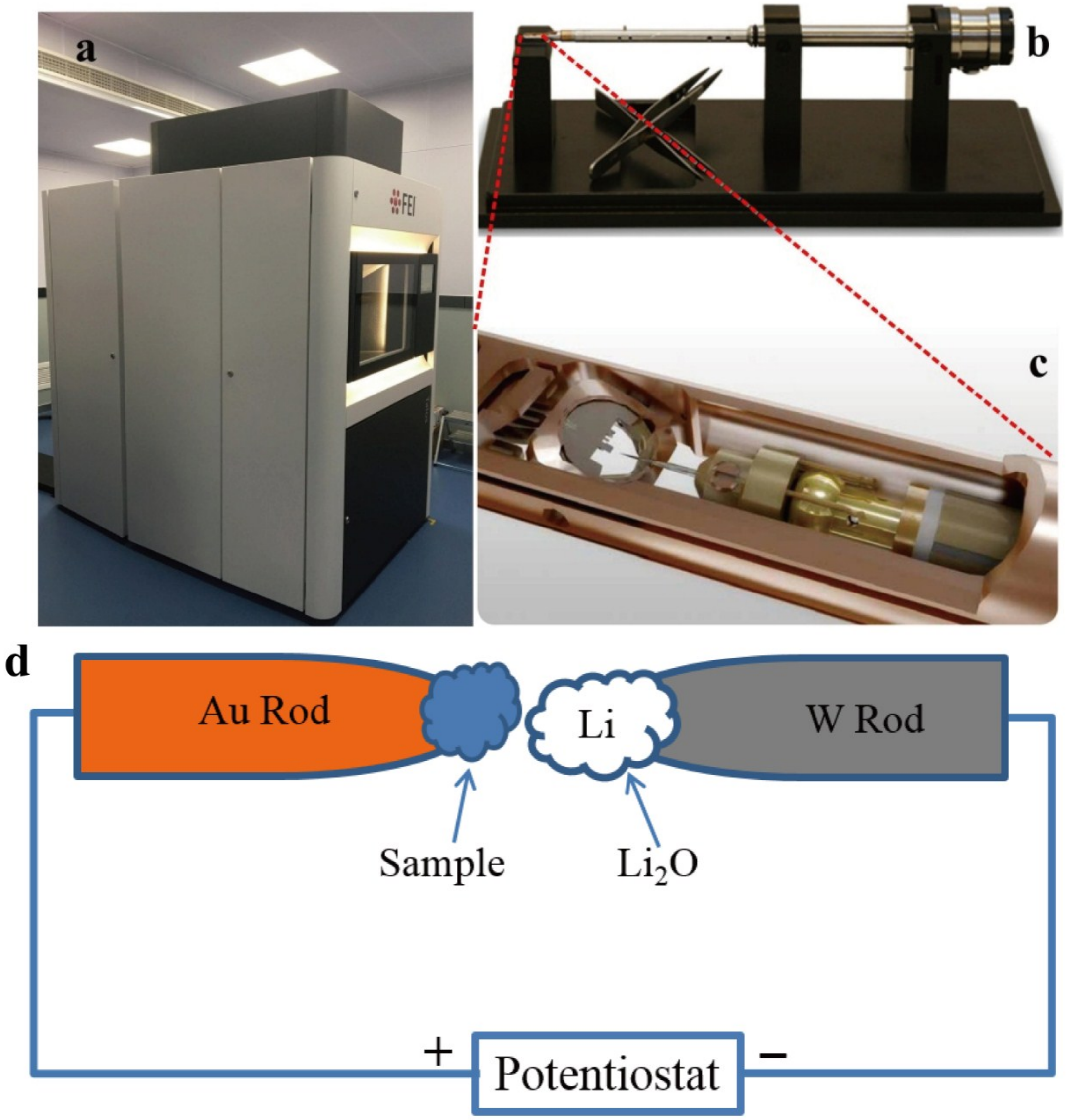

Figure S8. (a) FEI Talos 200S TEM. (b) *In-situ* TEM device and (c) the enlarged view. (d) schematics illustration of *in-situ* TEM test.

9. Home-built *in-situ* electrochemical NMR probe.

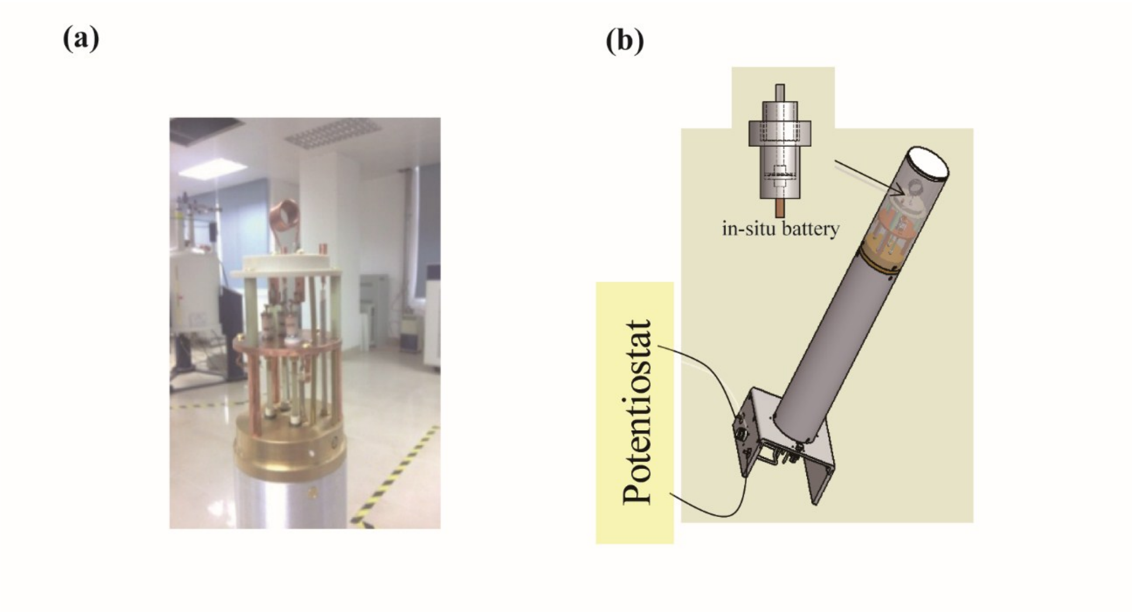

Figure S9. (a) Home-built *in-situ* electrochemical NMR probe. (b) Schematics illustration of *in-situ* NMR test.

10. Electronic conductivities of fluorinated graphene materials.

Table S1. Electronic conductivities of GF_x materials.

Samples	**Area (cm^2)**	**Thickness (cm)**	**R (Ω)**	**Conductivity (S/cm)**
GF1.1	3.14	0.008	1.78E+08	1.43E-11
GF0.8	3.14	0.004	1.35E+07	9.44E-11
GF0.5	3.14	0.006	3.60E+03	5.31E-07

The materials were firstly pressed into pieces under a certain pressure and then tested by EIS method. The results show that the conductivity of $GF_{0.5}$ is 3~4 orders of magnitude higher than that of $GF_{0.8}$ and $GF_{1.1.}$